Growth Kinetics of Silver Bromide Nanoparticles in Aqueous Nonionic Surfactant Solutions

ARTICLE *in* INDUSTRIAL & ENGINEERING CHEMISTRY RESEARCH · OCTOBER 2011

Impact Factor: 2.59 · DOI: 10.1021/ie2009247

2 AUTHORS, INCLUDING:

Santanu Paria
National Institute of Technology Rourkela
52 PUBLICATIONS **1,782** CITATIONS

SEE PROFILE

I&EC research
Industrial & Engineering Chemistry Research

ARTICLE

pubs.acs.org/IECR

Growth Kinetics of Silver Bromide Nanoparticles in Aqueous Nonionic Surfactant Solutions

Minaketan Ray and Santanu Paria*

Department of Chemical Engineering, National Institute of Technology, Rourkela 769 008, Orissa, India

ABSTRACT: The synthesis of silver bromide nanoparticles has been studied by many researchers because of their wide ranges of applications. This article reports on the growth kinetics of silver bromide nanoparticles in the presence and absence of aqueous nonionic surfactant media. The effects of different parameters such as the reactant concentration, the temperature, and the presence of a nonionic surfactant have also been studied. It was found that these parameters have significant effects on the process of growth kinetics, as well as on the equilibrium particle size. In pure aqueous media, the particle size decreases with increasing reactant concentration. The presence of nonionic surfactant (TX-100) significantly lowers the AgBr particle size compared to that obtained in pure aqueous media.

1. INTRODUCTION

Nanosized materials are of great interest in the fields of science and technology because of their superiority in physical, chemical, electronic, optical, and other properties over the corresponding bulk-scale materials. Nanoscale silver halide is getting increasing attention because of its promising applications in the fields of semiconductors,[1] antibacterial activity,[2,3] photographic materials,[4,5] dye adsorption studies,[5] and so on.

Although many studies are available on the preparation of silver halide nanoparticles,[6−13] there are limited studies on the kinetics of particle formation.[14,15] Studies on the kinetics of particle formation can provide important information about the nucleation and growth of the particles. Among the reported studies, different microemulsions have mostly been used as nanoreactors to control the particle size. Husein et al.[6,7,10] prepared silver chloride and silver bromide nanoparticles by the microemulsion method using dioctyldimethyl ammonium chloride, dioctyldimethyl ammonium bromide, and cetyltrimethyl ammonium bromide cationic surfactants. In this method, the counterions of the surfactants are used as the source of halide ion to give silver halide. Husein et al. also prepared AgCl and AgBr nanoparticles in microemulsions containing the cationic surfactants dioctyldimethylammonium chloride and cetyltrimethylammonium bromide from the respective solid powders of AgCl and AgBr.[8,9] Spirin et al.[14] studied the growth kinetics of AgI nanoparticles in sodium bis(2-ethylhexyl) sulfosuccinate (AOT) reverse microemulsions using oil phases with different chain lengths (*n*-hexane, *n*-octane, *n*-decane, *n*-dodecane). They found that, if the water/surfactant molar ratio (W) was low (∼2), there was no change in particle size on changing the chain length of the oil phase, but there was a significant change at higher values of W. In addition, lower particle sizes were obtained when the oil chain length was low.

Only limited studies on the growth kinetics of AgBr nanoparticles are available in the literature.[16−18] Moreover, to the best of our knowledge, similar studies on the growth kinetics of silver bromide nanoparticles both in pure aqueous media and in the presence of aqueous nonionic surfactant solutions are not available in the literature. In this study, we investigated the growth kinetics of silver bromide nanoparticles in aqueous solution in the presence of a nonionic surfactant. Different parameters such as reactant ($AgNO_3$) concentration, surfactant concentration, and temperature on the growth kinetics were also studied. The Lifshitz−Slyozov−Wagner (LSW) model was used to calculate the coarsening rate constant of AgBr nanoparticle formation in aqueous media, and the effects of different parameters on the rate constant are reported.

2. EXPERIMENTAL SECTION

2.1. Materials. Reagent-grade silver nitrate (99.9%) and potassium bromide (99.3%) were purchased from Rankem, New Delhi, India. The nonionic surfactant Triton X-100 (TX-100, laboratory grade, cat. no. 9002-93-1), obtained from Sigma-Aldrich, was used without any further purification. Ultrapure water of 18.2 MΩ·cm resistivity and pH 6.4−6.5 was doubly distilled again before use in all experiments.

2.2. Methods. Silver bromide nanoparticles were prepared by the simple precipitation reaction of silver nitrate with potassium bromide. Fresh silver nitrate solution was prepared and used for each experiment to avoid photooxidation of the $AgNO_3$ solution. In the absence of surfactants, $AgNO_3$ solution was added to potassium bromide solution under mixing using a cyclomixer to obtain AgBr nanoparticles in the aqueous solution. In the presence of surfactant, potassium bromide and surfactant solutions were mixed, and then silver nitrate solution was added under mixing. The temperature of the solution was maintained constant throughout the experiments using a water bath circulator. All solutions were sonicated before mixing for degasification; the samples were also sonicated in a sonication bath for ∼1 min just before the particle size analysis. The particle size (diameter) was analyzed by dynamic light scattering (DLS)

Received: April 29, 2011
Accepted: September 2, 2011
Revised: August 4, 2011
Published: September 03, 2011

dx.doi.org/10.1021/ie2009247 | *Ind. Eng. Chem. Res.* 2011, 50, 11601–11607

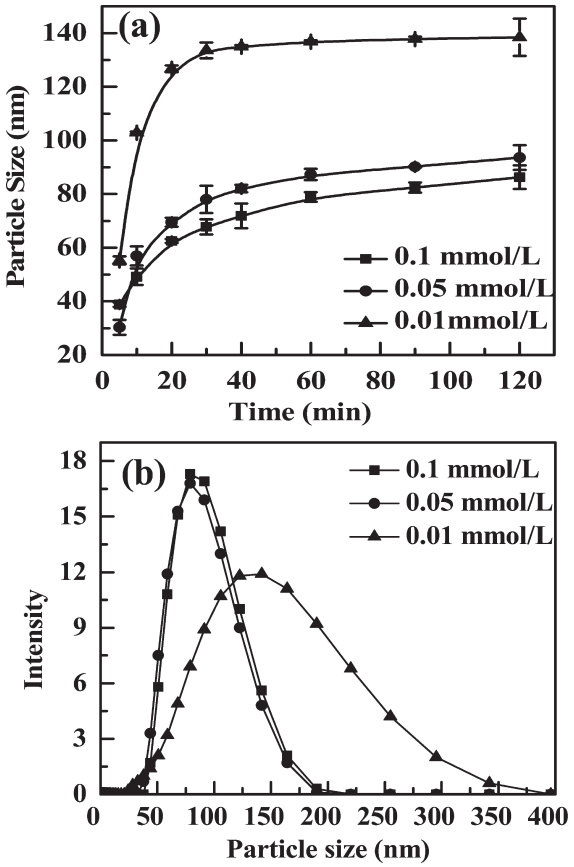

Figure 1. (a) Growth kinetics of AgBr nanoparticles using different reactant concentrations in aqueous media. (b) Distribution of AgBr nanoparticles measured by DLS.

technique using a Malvern Instruments analyzer (Nano ZS, Malvern, U.K.).

The kinetics of particle formation was also studied spectrophotometrically using a UV−vis−NIR spectrometer (UV-3600, Shimadzu, Kyoto, Japan). The particle shape and size were observed by scanning electron microscopy (SEM; JEOL, JSM-6480LV). The particles were also characterized using a Philips (PW 1830 HT) X-ray diffractometer at a scanning rate of 0.05° θ/s.

3. RESULTS AND DISCUSSION

3.1. Effect of Reactant Concentration on Equilibrium Time and Particle Size. The rate of change of particle size with time, or the growth kinetics, is an important phenomenon in any nanoparticle synthesis process. The formation of the equilibrium or final AgBr particle size depends on two steps: (i) the precipitation reaction of silver nitrate and bromide ions to form AgBr nuclei and (ii) the collision between the nuclei or diffusion of molecules to the nucleus surface and deposition to form the final particle size. The first step is controlled by the reaction, followed by growth. The first step can be very fast, as the reaction rate is high; as a result, the final particle size depends mainly on the growth process. First, the growth kinetics of AgBr particles was studied in aqueous media with varying $AgNO_3$ concentration. The results presented in Figure 1a show that the particle size gradually increased with time and ultimately reached equilibrium,

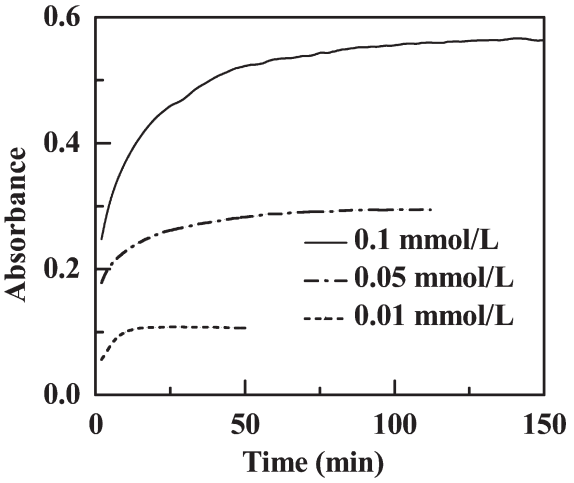

Figure 2. Growth kinetics of AgBr nanoparticles studied by UV−vis spectrophotometry at 270-nm wavelength in aqueous media using different reactant concentrations.

the equilibrium particle size increasing with decreasing reactant concentration among the three reactant concentrations studied here. Similarly, the equilibrium time also depended on the reactant concentration and decreased with decreasing reactant concentration. It was observed that the saturation times for 0.01, 0.05, and 0.1 mmol/L $AgNO_3$ concentrations were ~30, ~55, and ~60 min, respectively. Moreover, 60−70% of the equilibrium size was achieved within 10 min, after which there was a slight increase in size for all three concentrations. The particle size distributions, shown in Figure 1b, clearly indicate that, at lower reactant concentration, the distribution was wide. The growth kinetics studied by UV−vis spectroscopy also indicated similar trends with some differences in equilibrium time, as shown in Figure 2. No sharp UV absorbance peak was observed for AgBr particles in aqueous medium, so the change in UV absorbance with time at 270-nm wavelength was noted for the kinetic study. The changes in absorbance were very significant among the three different reactant concentrations studied here. The equilibrium times in UV−vis spectroscopy studies were ~20, ~50, and ~70 min for 0.01, 0.05, and 0.1 mmol/L concentrations, respectively, at a constant wavelength of 270 nm. Although there were some similarities between the UV and DLS results, the UV−vis spectroscopy study was still carried out, as the nucleation step is very fast and it is difficult to study the change in size at lower time scales using DLS. The UV results presented in Figure 2 indicate that the initial sharp increasing portion of the plot is the nucleation region, followed by the slowly increasing region of the growth zone.

It is well-known that the reactant concentration plays a crucial role in the final particle size of a nanoparticle synthesis process. In this study, the effect of reactant concentration on the equilibrium particle size indicated that the particle size decreased with increasing reactant concentration. The previously reported studies suggested that the effect of increasing reactant concentration on the size of the generated nanoparticles did not follow a particular trend, whereas increasing[19,20] or decreasing[21,22] trends were reported depending on the types of particles, synthesis media, and so on; in general, increasing size is quite common. When more than one reactant is present, at low reactant concentration, the number of nuclei formed will be lower, possibly because of a low reaction rate. In such a situation, the atoms form

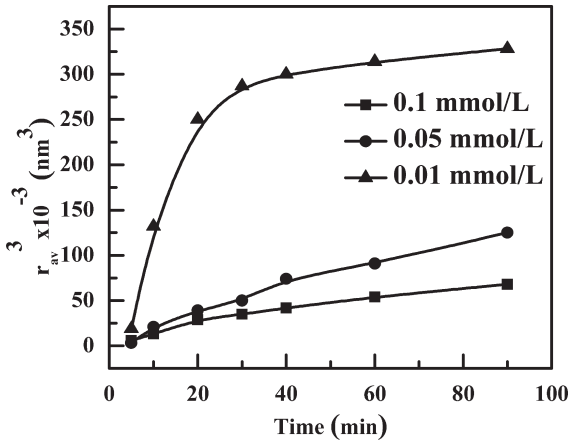

Figure 3. Plot of the cube of the radius versus time for AgBr nanoparticles prepared in aqueous media.

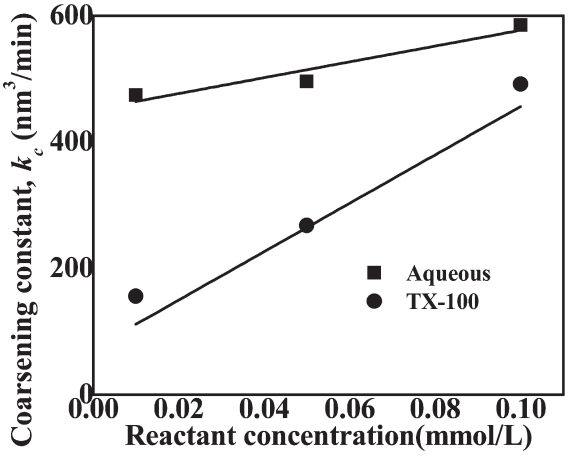

Figure 4. Plot of the coarsening constant with increasing reactant concentration in pure aqueous and TX-100 media.

embryos at later periods of reaction that collide with the already formed nuclei instead of forming new nuclei, leads to the formation of larger particles. In contrast, when the reactant concentration is increased, the concentration (number per unit volume) of nuclei also increases in the reaction medium because of both an increase in the reaction rate and the presence of more molecules, leading to the formation of smaller particles. Additionally, the solubility of AgBr in aqueous media also decreases when the concentration of $AgNO_3$ is increased because of the presence of a common ion (Ag^+). In this situation, as soon as the reaction is over, the transition of the embryo state to a nucleus is faster and favorable during the particle formation process. Ultimately, the final particle size becomes low because of the formation of more nuclei in the reaction medium. The equilibrium particle sizes obtained from DLS data in this work were 137 ± 1, 90 ± 2, and 83 ± 2 nm for 0.01, 0.05, and 0.1 mmol/L concentrations of reactant, respectively.

According to the Lifshitz−Slyozov−Wagner (LSW) model, the coarsening kinetics can be written as[23]

$$r_{av}^3 - r_0^3 = k_c t \quad (1)$$

where r_{av} and r_0 are the average and initial particle radii, respectively; k_c is the diffusion-limited coarsening rate constant; and t is the time. Figure 3 shows a plot of r_{av}^3 versus time. The

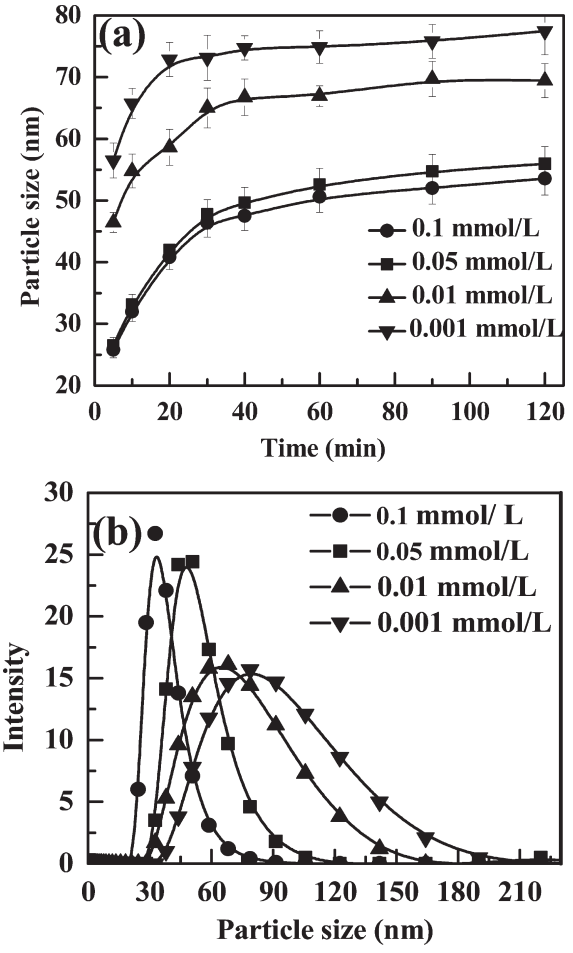

Figure 5. (a) Growth kinetics of AgBr nanoparticles in TX-100 media using different reactant concentrations. (b) Distribution of AgBr nanoparticles measured by DLS.

increasing particle size at longer times is attributed to diffusion-limited coarsening. The coarsening rate constant (k_c) can be obtained from the slope of eq 1 at higher time scales. Figure 4 shows a plot of the coarsening rate constant as a function of the reactant concentration. The coarsening rate constant increased almost linearly with the increase in the reactant concentration. One can clearly see that the value of k_c in the presence of TX-100 was always lower than that in the pure aqueous solution. This behavior can be explained as resulting from the formation of an adsorbed layer of surfactant molecules (TX-100) on the AgBr particles, preventing their growth and leading to a lower growth rate.

3.2. Effect of Surfactant. The nature of the surfactants and their structures also greatly influence the growth rate, equilibrium size, zeta potential, and stability of the particles. Herein, the effects of the nonionic surfactant TX-100 on the particle size and growth rate were studied. The effects of reactant concentration were also studied in the presence of TX-100 using concentrations of 0.001, 0.01, 0.05, and 0.1 mmol/L, as shown in Figure 5a. The surfactant concentration used was 0.45 mmol/L [3 times the critical micelle concentration (CMC)]. As in pure aqueous solution, it was observed that the particle size decreased with increasing reactant concentration, and the overall particle size was lower than that in pure aqueous media. At equilibrium, the particle sizes prepared using 0.01 mmol/L $AgNO_3$ in the presence and absence of surfactant were 70 ± 3 and 137 ± 1 nm, respectively. The presence of nonionic surfactant

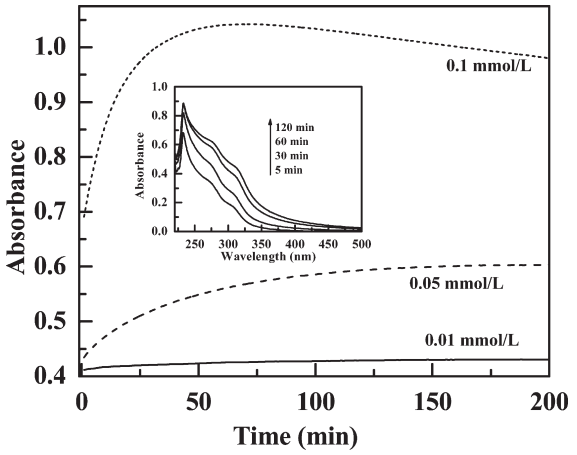

Figure 6. Growth kinetics of AgBr nanoparticles studied by UV−vis spectroscopy in TX-100 media using different reactant concentrations at 238 nm. Inset: Full UV spectra at different times from 0.1 mmol/L reactant concentration.

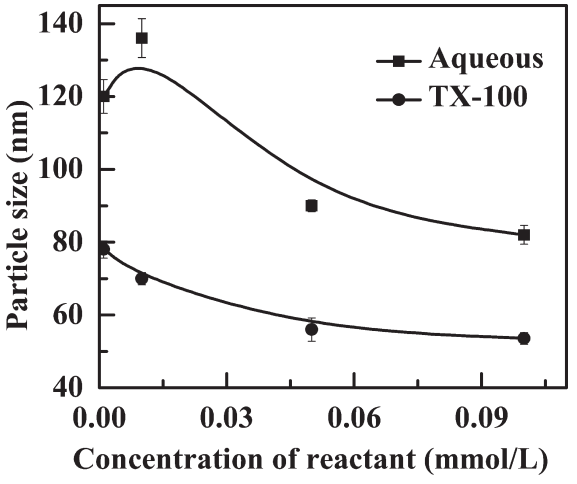

Figure 7. Change in equilibrium particle size of AgBr nanoparticles with increasing reactant concentration in pure aqueous and TX-100 media.

TX-100 decreased the equilibrium time (30 min) in addition to lowering of particle size. As in pure aqueous media, the values of k_c increased linearly with the reactant concentration, and lower k_c values were obtained in the presence of TX-100, as shown in Figure 4. Apart from the smaller size, the size distribution was also narrower at higher reactant concentration, as shown in Figure 5b. The effects of surfactant concentration on the equilibrium particle size over a wide range, from below to above the CMC, were studied, and it is observed that, in the presence of TX-100, the change in particle size with changing surfactant concentration was negligible.

The kinetics of particle growth in the presence of surfactants was also studied using UV−vis spectrophotometry. In the presence of surfactant, the peak at the maximum absorbance value shifted to lower wavelength, possibly because of the adsorption of surfactant on the particle surface. The UV spectrum of AgBr nanoparticles in the presence of TX-100 solution was obtained with a maximum absorbance at 238-nm wavelength. Figure 6 shows that the absorbance value increased gradually with time and reached to a plateau after 30 min using a constant $AgNO_3$ (0.1 mmol/L) concentration. The effect of reactant concentration

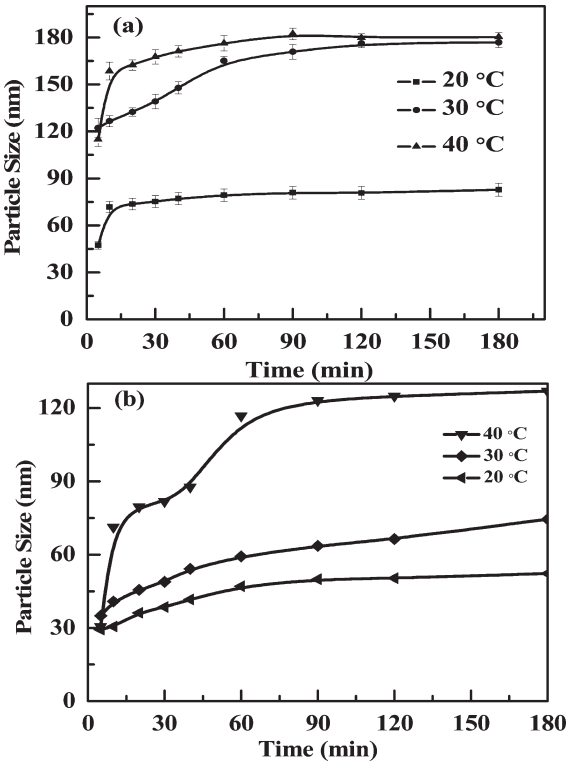

Figure 8. Growth kinetics of AgBr nanoparticles at different temperatures for 0.1 mmol/L $AgNO_3$ concentration: (a) pure aqueous and (b) TX-100 media.

was also studied using the three different concentrations 0.01, 0.05, and 0.1 mmol/L $AgNO_3$ in the presence of TX-100 at 238-nm wavelength. The absorbance value increased gradually with time and finally reached a plateau region at equilibrium; also, there was an increase in absorbance value with increasing reactant concentration. The increase in absorbance with the reactant concentration can be attributed to the decrease in particle size in the medium, which, in turn, led to an increase in particle density.

Figure 7 depicts the change in equilibrium particle size with reactant concentration in the presence and absence of surfactant. In pure aqueous media at very low reactant concentration, initially, there was a slight increase in particle size with increasing reactant concentration. Above 0.01 mmol/L concentration, there was a gradual decrease in particle size with increasing reactant concentration. Thus, the increase in particle size at lower reactant concentration can be attributed to the presence of fewer nuclei in the reaction medium, as explained before. When the reactant concentration is very low, fewer nuclei can form. Under such conditions, when there is a further slight increase in reactant concentration, newly formed AgBr molecules are deposited on the existing nuclei instead of forming new ones; as a result, an increase in particle size is observed. In contrast, in the presence of TX-100, a gradual decrease in particle size was observed.

3.3. Effect of Temperature. The effects of temperature on the growth kinetics and equilibrium particle size were studied in aqueous media in the presence and absence of surfactant solutions at different temperatures (20, 30, and 40 °C). The moderate temperature range was selected because the solubility of the surfactant can decrease at low temperature and the solution might also reach the cloud point at higher temperature. The effects of temperature on the growth kinetics of silver bromide nanoparticles

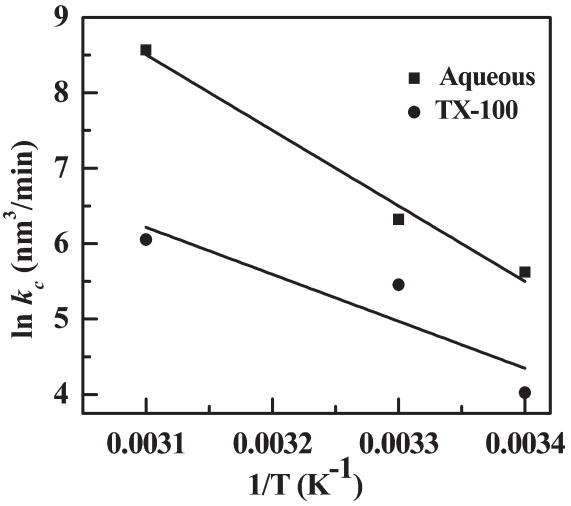

Figure 9. Plot of ln k_c versus T^{-1} in pure aqueous and TX-100 media.

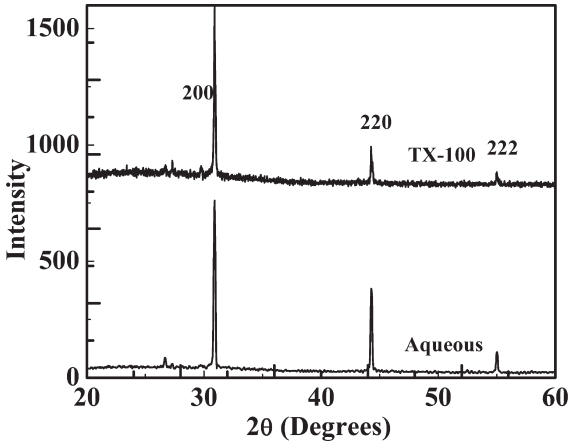

Figure 10. Powder X-ray diffraction patterns of AgBr nanoparticles synthesized in pure aqueous and TX-100 media.

are presented in Figure 8. It can be observed that, in both the presence and absence of surfactant, the particle size and equilibrium time increased with increasing temperature. Because the kinetic energy of the system increased with increasing temperature, the probability of collision between the nanoparticles also increased. The collisions between the particles, in turn, enhanced the growth rate and led to the formation of larger nanoparticles. In addition, after the formation of particle nuclei, growth also proceeded because of the diffusion of the molecules from the aqueous phase to the nucleus surface. At higher temperatures, the diffusion-controlled growth rate increased because of the increase in diffusion rate. In aqueous solution, there was a sharp increase in particle size as the temperature was increased from 20 to 30 °C. In contrast, when the temperature was increased to 40 °C, there was no such change in the particle growth. However, in the presence of TX-100, between 20 and 30 °C, the change was not significant, but there was a significant difference with the increase to 40 °C. This behavior can be attributed to the adsorbed surfactant layer on the particle surface resisting particle−particle collisions, but collisions being favored at higher temperature (40 °C), leading to an increase in particle size. Additionally, for a significant change in

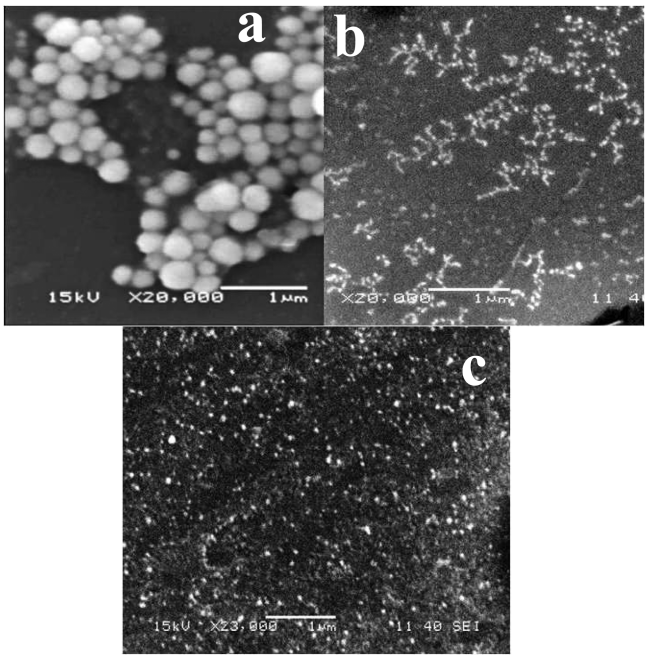

Figure 11. SEM images of AgBr nanoparticles obtained using (a) 0.01 mmol/L $AgNO_3$, (b) 0.1 mmol/L $AgNO_3$, and (c) 0.01 mmol/L $AgNO_3$ in the presence of TX-100.

temperature, the adsorption density of the surfactant on the particle surface could also decrease, which would favor collisions and lead to an increase in particle size.

According to the Arrhenius equation, the coarsening rate constant is related to the temperature and activation energy as

$$k_c = Ae^{-E_a/RT} \quad \text{or} \quad \ln k_c = -\frac{E_a}{RT} + \ln A \tag{2}$$

where E_a is the activation energy for the growth process, A is the pre-exponential constant, R is the universal gas constant, and T is the temperature (in kelvin). The activation energy of the coarsening process can be calculated from slope of a plot of ln k_c versus T^{-1}, as shown in Figure 9. The activation energy values obtained from the plot are 83.29 ± 3.4 kJ/mol for aqueous solutions and 77.67 ± 2.31 kJ/mol for surfactant solutions. The activation energies obtained are comparable to the reported values for other hydrophilic particles such as TiO_2 (72.36 kJ/mol),[24] ZnO (108 kJ/mol),[25] and silicalite-1 (73.90 ± 2.80 kJ/mol).[26]

The coarsening constant, k_c, can be also written as

$$k_c = \frac{8\gamma D V_m{}^2 C_\infty}{9RT} \tag{3}$$

where γ is the surface energy of AgBr (J/m^2), D is the diffusivity of AgBr nanoparticles, V_m is the molar volume (28.9 cm^3/mol),[27] C_∞ is the AgBr concentration, R is the universal gas constant [8.31 J/(mol·K)], and T is the working temperature (300 K). The bulk diffusivity of the silver bromide nanoparticles can be calculated using the Stokes−Einstein equation as[28]

$$D = \frac{k_B T}{6\pi\eta a} \tag{4}$$

where k_B is the Boltzmann constant (1.38×10^{-23} J/K), η is the viscosity of the medium [8.38×10^{-4} kg/(m·s)],[29] and a is the hydrodynamic radius (0.264 nm)[30] of the AgBr molecule.

The calculated surface energy of AgBr nanoparticles using 0.01 mmol/L $AgNO_3$ concentration is 219 mJ/m^2. This value of the surface energy is comparable to the previously reported values of 91.5−188 mJ/m^2.[31]

3.4. Particle Characterization by XRD and SEM. The synthesized particles were also characterized by XRD, and the pattern of the AgBr nanoparticles is presented in Figure 10. The peaks of the XRD spectrum are clearly distinguishable. The XRD pattern of AgBr in both surfactant and aqueous media display three main peaks located at 30.8°, 44.2°, and 54.9°, corresponding to the (200), (220) and (222) planes, respectively (JPCDS card no. 79-0149). The most intense peak was obtained for the (200) plane. The peaks were slightly narrower in surfactant media, indicating higher crystallinity than the pure aqueous media.

The SEM images of AgBr nanoparticles obtained using 0.01 and 0.1 mmol/L reactant concentration in aqueous solution and 0.01 mmol/L reactant concentration in the presence of TX-100 are shown in parts a−c, respectively, of Figure 11. It can be clearly seen that the particles are mostly spherical in shape. Comparison between parts a and b of Figure 11 shows that, with the increase in concentration from 0.01 to 0.1 mmol/L, there was a decrease in particle size, as discussed before. Comparison between parts a and c of Figure 11 also shows that the presence of TX-100 generated smaller particles than the pure aqueous media. The fact that the particle size obtained by DLS in the presence of surfactant was larger than that obtained by SEM might be because of the adsorbed surfactant layer, as well as hydrated water molecules.

4. CONCLUSIONS

Spherical AgBr nanoparticles were prepared in aqueous media in the absence and presence of surfactant. Smaller particles were obtained in pure aqueous media by increasing the reactant concentration. The coarsening rate constant for the particle formation was found to increase linearly with increasing reactant concentration. The presence of nonionic surfactant generated smaller particles than were obtained in pure aqueous media. The coarsening rate constant in the presence of TX-100 was always lower than that in the presence of pure aqueous media. In pure aqueous media, the temperature effect caused an increase in particle size as the temperature was increased from 20 to 30 °C, after which the change was not significant. In contrast, in the presence of TX-100, the change was not significant in the 20−30 °C temperature range, but a further increase to 40 °C resulted in a significant change in size.

AUTHOR INFORMATION

Corresponding Author

*E-mail: santanuparia@yahoo.com or sparia@nitrkl.ac.in. Fax: +91 661 246 2999.

ACKNOWLEDGMENT

Financial support from the Department of Science and Technology (DST) under Nanomission, New Delhi, India, Grant SR/S5/NM-04/2007, for this project is gratefully acknowledged. M.R. thanks DST, India, for the Senior Research Fellowship.

REFERENCES

(1) Baetzold, R. C. Molecular Orbital Description of the Metal−Semiconductor Interface Ag−AgBr. *J. Solid State Chem.* **1973**, *6*, 352.

(2) Sambhy, V.; MacBride, M.; Peterson, B. R.; Sen, A. Silver Bromide Nanoparticle/Polymer Composites: Dual Action Tunable Antimicrobial Materials. *J. Am. Chem. Soc.* **2006**, *128*, 9798.

(3) Elahifard, M. R.; Rahimnejad, S.; Haghighi, S.; Gholami, M. R. Apatite-Coated Ag/AgBr/TiO_2 Visible-Light Photocatalyst for Destruction of Bacteria. *J. Am. Chem. Soc.* **2007**, *129*, 9552.

(4) Sturmer, D. M.; Marchetti, A. P.; Sturge, J.; Waworth, V.; Shepp, A. *Imaging Processes and Materials*, 8th ed.; Wiley: New York, 1989; p 71.

(5) Jeunieau, L.; Alin, V.; Nagy, J. B. Adsorption of Thiacyanine Dyes on Silver Halide Nanoparticles: Study of the Adsorption Site. *Langmuir* **2000**, *16*, 597.

(6) Husein, M. M.; Rodil, E.; Vera, J. H. Formation of Silver Chloride Nanoparticles in Microemulsions by Direct Precipitation with the Surfactant Counterion. *Langmuir* **2003**, *19*, 8467.

(7) Husein, M. M.; Rodil, E.; Vera, J. H. Formation of Silver Bromide Precipitate of Nanoparticles in a Single Microemulsion Utilizing the Surfactant Counterion. *J. Colloid Interface Sci.* **2004**, *273*, 426.

(8) Husein, M. M.; Rodil, E.; Vera, J. H. A Novel Method for the Preparation of Silver Chloride Nanoparticles Starting from Their Solid Powder Using Microemulsions. *J. Colloid Interface Sci.* **2005**, *288*, 457.

(9) Husein, M. M.; Rodil, E.; Vera, J. H. A Novel Approach for the Preparation of AgBr Nanoparticles from their Bulk Solid Precursor Using CTAB Microemulsions. *Langmuir* **2006**, *22*, 2264.

(10) Husein, M. M.; Rodil, E.; Vera, J. H. Preparation of AgBr Nanoparticles in Microemulsions via Reaction of $AgNO_3$ with CTAB Counterion. *J. Nanopart. Res.* **2007**, *9*, 787.

(11) Oleshko, V. P. Size Confinement Effects on Electronic and Optical Properties of Silver Halide Nanocrystals as Probed by Cryo-EFTEM and EELS. *Plasmonics* **2008**, *3*, 41.

(12) Bai, J.; Li, Y.; Zhang, C.; Liang, X.; Yang, Q. Preparing AgBr Nanoparticles in Poly(vinyl pyrrolidone) (PVP) Nanofibers. *Colloids Surf. A* **2008**, *329*, 165.

(13) Liu, X. H.; Luo, X. H.; Lu, S. X.; Zhang, J. C.; Cao, W. L. A Novel Cetyltrimethyl Ammonium Silver Bromide Complex and Silver Bromide Nanoparticles Obtained by the Surfactant Counterion. *J. Colloid Interface Sci.* **2007**, *307*, 94.

(14) Spirin, M. G.; Brichkin, S. B.; Razumov, V. F. Growth Kinetics for AgI Nanoparticles in AOT Reverse Micelles: Effect of Molecular Length of Hydrocarbon Solvents. *J. Colloid Interface Sci.* **2008**, *326*, 117.

(15) Hasse, U.; Fletcher, S.; Scholz, F. Nucleation-Growth Kinetics of the Oxidation of Silver Nanocrystals to Silver Halide Crystals. *J. Solid State Electrochem.* **2006**, *10*, 833.

(16) Sugimoto, T. Stable Crystal Habits of General Tetradecahedral Microcrystals and Monodisperse AgBr Particles: I. Equilibrium Forms and Steady Forms. *J. Colloid Interface Sci.* **1983**, *91*, 51.

(17) Sugimoto, T. Stable Crystal Habits of General Tetradecahedral Microcrystals and Monodisperse AgBr Particles. II. Steady Forms in Open Systems. *J. Colloid Interface Sci.* **1983**, *93*, 461.

(18) Sugimoto, T. The Theory of the Nucleation of Monodisperse Particles in Open Systems and its Application to AgBr Systems. *J. Colloid Interface Sci.* **1992**, *150*, 208.

(19) Sugimoto, T.; Shiba, F. Spontaneous Nucleation of Monodisperse Silver Halide Particles from Homogeneous Gelatin Solution II: Silver Bromide. *Colloids Surf. A* **2000**, *164*, 205.

(20) Mafune, F.; Kohno, J.; Takeda, Y.; Kondow, T. Structure and Stability of Silver Nanoparticles in Aqueous Solution Produced by Laser Ablation. *J. Phys. Chem. B* **2000**, *104*, 8333.

(21) Pal, T.; Sau, T. K.; Jana, N. R. Reversible Formation and Dissolution of Silver Nanoparticles in Aqueous Surfactant Media. *Langmuir* **1997**, *13*, 1481.

(22) Pawar, M. J.; Chaure, S. S. Synthesis of CdS Nanoparticles Using Glucose as Capping Agent. *Chalcogenide Lett.* **2009**, *12*, 689.

(23) Rao, C. N. R.; Muller, A.; Anthony, K. *Nanomaterials Chemistry: Recent Developments and New Directions*; Wiley-VCH: New York, 2007; pp 141−145.

(24) Oskam, G.; Nellore, A.; Penn, R. L.; Searson, P. C. The Growth Kinetics of TiO_2 Nanoparticles from Titanium(IV) Alkoxide at High Water/Titanium Ratio. *J. Phys. Chem. B* **2003**, *107*, 1734.

(25) Hu, Z.; Escamilla Ramírez, D. J.; Heredia Cervera, B. E.; Oskam, G.; Searson, P. C. Synthesis of ZnO Nanoparticles in 2-Propanol by Reaction with Water. *J. Phys. Chem. B* **2005**, *109*, 11209.

(26) Cheng, C. H.; Shantz, D. F. Silicalite-1 Growth from Clear Solution: Effect of the Alcohol Identity and Content on Growth Kinetics. *J. Phys. Chem. B* **2005**, *109*, 19116.

(27) Grammatikakis, J.; Papathanassiou, A. N. Prediction of the Pressure Derivative of the Adiabatic Bulk Modulus of AgBr:AgCl. *J. Phys. Chem. Solids* **1992**, *53*, 1251.

(28) Hiemenz, P. C.; Rajagopalan, R. *Principles of Colloid and Surface Chemistry*, 3rd ed.; CRC Press: Boca Raton, FL, 1997.

(29) Terpilowski, K.; Holysz, L.; Chibowski, E. Surface Free Energy of Sulfur—Revisited: II. Samples Solidified Against Different Solid Surfaces. *J. Colloid Interface Sci.* **2008**, *319*, 514.

(30) Mariano, N. C.; Schelly, Z. A. Dynamics of Electroporation of Synthetic Liposomes Studied Using a Pore-Mediated Reaction, $Ag^+ + Br^- \rightarrow AgBr$. *J. Phys. Chem. B* **1998**, *102*, 9319.

(31) Sugimoto, T. *Monodispersed Particles*; Elsevier: Amsterdam, 2001; pp 17−24.